Catalysis Today 160 (2011) 198–203

Contents lists available at ScienceDirect

Catalysis Today

journal homepage: www.elsevier.com/locate/cattod

Interaction of water with the clean and oxygen pre-covered Ir(1 1 1) surface☆

Ming Pan, Son Hoang, C. Buddie Mullins*

Departments of Chemical Engineering and Chemistry, Center for Nano- and Molecular Science and Technology, Texas Materials Institute, and Center for Electrochemistry, University of Texas at Austin, Austin, TX 78712-0231, USA

ARTICLE INFO

Article history:
Available online 9 June 2010

Keywords:
Ultrahigh vacuum
Ir(1 1 1) single crystal
Water dissociation
Adsorption
Desorption
Temperature programmed desorption
Oxygen
Apparent activation energy

ABSTRACT

Adsorption and reaction of water on the clean and oxygen modified Ir(1 1 1) single crystal surfaces have been studied using temperature programmed desorption (TPD) and molecular beam reactive scattering (MBRS) techniques under ultrahigh vacuum (UHV) conditions. Water dissociates on the clean Ir(1 1 1) surface with a probability (estimated based on production of hydrogen) which decreases from ~0.016 to 0.004 ± 0.0015 with increasing water coverages from 0.34 to 2.59 monolayer. Scattering experiments performed at various surface temperatures in the limit of zero coverage yield water dissociation probabilities in the range of ~0.0005–0.012 (300–900 K) with an uncertainty expressed as ±20% of the dissociation probability. The apparent activation energy for water dissociation on clean Ir(1 1 1) is estimated to be ~170 ± 5 kJ/mol employing MBRS techniques, which probably cannot be applied to TPD measurements with higher water coverages. We speculate that water dissociation occurs on the defects of the Ir(1 1 1) surface. Using isotopically labeled reactants, a strong interaction between adsorbed water and oxygen was found on Ir(1 1 1), indicated by a new water desorption feature at 235 K and scrambled oxygen and water desorption products.

© 2010 Elsevier B.V. All rights reserved.

1. Introduction

Water is involved in numerous catalytic processes such as the water–gas shift (WGS) reaction [1,2] and methane reforming [3,4]. Thus, studies on the interaction of water with metal surfaces are of fundamental importance for understanding reaction mechanisms. Regarding adsorption, dissociation and desorption of water, many transition metals (e.g. Ru [5–7], Pt [8,9], Zr [10], Ni [11], Pd [12], Rh [13,14], Cu [15], Ag [16], and Au [17]) have been investigated both experimentally and theoretically. Furthermore, it has been found that co-adsorbed oxygen can induce the dissociation of water on some metal surfaces with hydroxyl groups (OH) as intermediates in the process [18–22]. These findings have provided deeper insight into reactions involving water. Ojifinni et al. and Kim et al. found that water can enhance CO oxidation on the Au(1 1 1) surface under ultrahigh vacuum (UHV) conditions employing isotopically labeled reactants [23,24], and a similar phenomenon has been observed on Pt(1 1 1) [25]. Water enhancement has also been found in CO oxidation on Au/TiO_2 [26,27] and the oxidation of propylene to propylene oxide on Ag(1 1 0) [28]. Additionally, Pan et al. noticed that adsorbed water alone or co-adsorbed water and oxygen can induce CO dissociation on Ir(1 1 1) [29].

Although iridium has been investigated widely with respect to its chemical properties [30–37] due to its high reactivity, the interaction of water with the clean or oxygen modified Ir(1 1 1) surface has yet to be a focus of interest. However, Weinberg and co-workers used TPD to investigate the adsorption of water on Ir(1 1 0) and found that at most 6% could dissociate at 130 K and hydroxyl formation occurred when water was co-adsorbed with oxygen on Ir(1 1 0) [38]. It is well known that the (1 1 1) facet is most readily formed in classical heat-treated catalysts due to its high stability. Here we present results demonstrating that water dissociates on the clean Ir(1 1 1) surface, and that co-adsorbed oxygen can strongly enhance water dissociation via hydroxyl group formation.

2. Experimental

All experiments were carried out in an ultrahigh vacuum (UHV) supersonic molecular beam surface scattering apparatus with a base pressure of ~2×10^{-10} Torr, which has been described [39–43] in detail previously, but particularly relevant aspects are provided here. This instrument consists of a UHV scattering/analysis section and a differentially pumped molecular beam generating section. The scattering chamber is equipped with an Auger electron spectrometer (AES), low energy electron diffraction optics (LEED), and

☆ This paper is for a special issue entitled "Heterogeneous Catalysis by Metals: New Synthetic Methods and Characterization Techniques for High Reactivity" guest edited by Jinlong Gong and Robert Rioux.

* Corresponding author. Tel.: +1 512 471 5817; fax: +1 512 471 7060.
E-mail address: mullins@che.utexas.edu (C.B. Mullins).

0920-5861/$ – see front matter © 2010 Elsevier B.V. All rights reserved.
doi:10.1016/j.cattod.2010.05.008

a quadrupole mass spectrometer (QMS). The Ir(1 1 1) single crystal sample is in the shape of a disk of ~1 cm diameter, mounted on a probe which can be adjusted in the *X*, *Y*, and *Z* directions and rotated by a sample manipulator. The Ir(1 1 1) sample can be resistively heated to 1550 K and rapidly cooled to 77 K via coupling to a liquid nitrogen (LN_2) bath. A type-C thermocouple (5%-W/Re/26%-W/Re) is spot-welded on the edge of the crystal and employed to measure the sample temperature. Research purity $^{16}O_2$ and $H_2{}^{16}O$ were used in this study, as were isotopically labeled D_2O and $H_2{}^{18}O$, to investigate the reaction pathways. All reagents can be delivered to the scattering chamber via molecular beams, which are generated using a system of independent nozzles, each with the same aperture size and separate plumbing to ensure the purity of reagents introduced to the sample surface. The oxygen coverage was determined by LEED measurements on an oxygen saturated surface and the results are in agreement with those that have been reported previously [44]. Water was dosed via molecular beam on the sample with a flux of ~0.08 monolayer (ML)/s and we estimate the surface density of 1 ML water to be $\sim 1.23 \times 10^{15}$ molecules/cm^2 by analogy with the water structure on the Pt(1 1 1) surface [45]. An inert stainless steel flag is installed in front of the sample for the control experiments to investigate the perturbing effects due to surfaces other than sample, such as the inner walls of the chamber, sample supporting wires, power leads, and the liquid nitrogen cooled sample probe. Periodically, the sample was cleaned by Ar ion sputtering, followed by annealing in gaseous oxygen. More routine cleaning, which must be carried out before every experiment, was performed with several cycles of oxygen adsorption/desorption to remove surface carbon as verified by AES and TPD measurements.

3. Results and discussion

3.1. Complete dissociation of water on clean Ir(1 1 1)

Complete dissociation of water on the clean Ir(1 1 1) surface was investigated by adsorbing water on the clean Ir(1 1 1) surface to search for hydrogen formation. We employed isotopically labeled water (D_2O) to eliminate the perturbing effects of background H_2 [due to the thermal dissociation of background H_2O and hydrocarbons (from a small component of fluid vapor from the LN_2 trapped diffusion pump) on hot filaments and diffusion from the stainless steel chamber walls] by monitoring D_2 production from Ir(1 1 1), which is one indicator of complete dissociation of water. Therefore, Fig. 1 shows the TPD spectra of D_2 ($m/e = 4$) desorption from Ir(1 1 1) covered by D_2O (0–2.59 ML) in a broad feature from ~200 to 700 K, indicating low temperature water dissociation (<200 K). The desorption rate of D_2 reached a maximum value at ~350–400 K, consistent with characteristic features regarding hydrogen desorption from Ir(1 1 1) [46]. Compared to the control experiment (we ramped the temperature of the clean sample up to 700 K at the same rate, 2 K/s) shown as the black curve, notable amounts of D_2 are produced from D_2O covered Ir(1 1 1) which suggest water dissociation on the clean Ir(1 1 1) surface. Additionally, when we dosed water on the inert stainless flag and then conducted TPD measurements, no mass 4 signal was detected, further suggesting that Ir(1 1 1) is responsible for water dissociation rather than other surfaces (i.e., copper power leads, tantalum sample-holding wires, and/or thermocouple wires). We estimate that the D_2O dissociation probability increases from ~0.004 to 0.016 ± 0.0015 with D_2O coverages decreasing from 2.59 to 0.34 ML [we also accounted for mass 3 (HD), which is due to the combination of background H and D from dissociated D_2O]. Note that the estimation of water dissociation probability is based on the TPD measurements from saturated hydrogen (1 ML) covered Ir(1 1 1), which is difficult to conduct due to the low dissociation probability of hydrogen on Ir(1 1 1) (~7×10^{-3} [46]) and could be the main source of uncertainty. The inset graph in Fig. 1 represents the modified production of D_2 [i.e., sum of integrated D_2 and half of the HD intensity], initially increasing as a function of increasing D_2O coverages and then leveling off when more than 1 ML of water was adsorbed on Ir(1 1 1). This observation is likely due to a decrease in surface active sites which are eventually occupied by absorbed water molecules until fully covering the Ir(1 1 1) surface and inhibiting the further dissociation of water.

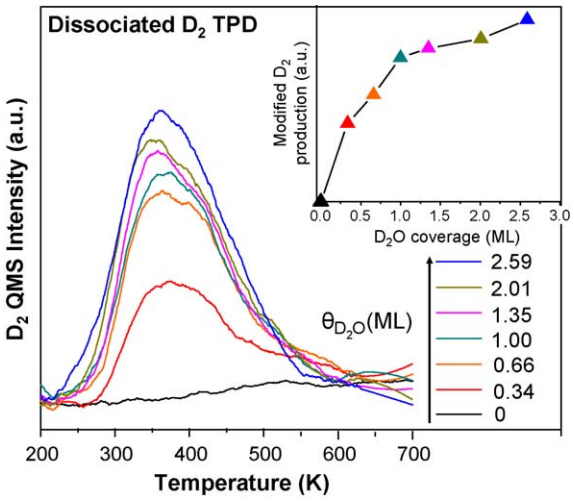

Fig. 1. TPD spectra of D_2 desorption from D_2O covered Ir(1 1 1) with various coverages. Inset graph shows the modified D_2 production with respect to integrated TPD areas of D_2 and HD where the data dots are filled by responding colors. Water was dosed on the surface between 89 and 77 K and the heating rate was 2 K/s. (For interpretation of the references to colour in this figure legend, the reader is referred to the web version of the article.)

In order to further study the thermal dissociation of water, we investigated the influence of surface temperature by employing molecular beam reactive scattering (MBRS) techniques. We impinged a D_2O beam on Ir(1 1 1) at a variety of surface temperatures above that for water desorption (from 300 to 900 K with an interval of 100 K as shown in Fig. 2a) and found that higher surface temperatures produced more D_2, indicating water dissociation on Ir(1 1 1) is activated [47]. We note that for all temperatures the production of D_2 initially increases to a peak value and then declines until reaching a steady state. The highest intensity is the maximum D_2 formation rate (R_{max}) for a given surface temperature. By comparing R_{max} as a function of temperature, an Arrhenius plot has been produced as shown in Fig. 2b resulting in an apparent activation energy for water dissociation (assuming water dissociation is the rate limiting step) on Ir(1 1 1) of $\sim 170 \pm 5$ kJ/mol. This is an overall activation energy including the two steps in complete water dissociation: water dissociates to a hydroxyl group and hydrogen atom ($H_2O \rightarrow OH + H$); the formed hydroxyl group then dissociates to oxygen and hydrogen ($OH \rightarrow H + O$). Using density functional theory calculations, Mavrikakis and co-workers [48] reported that complete water dissociation on Pt(1 1 1) has an activation energy barrier of 1.97 eV including 0.88 eV in water dissociation to OH and H and 1.09 eV in OH dissociation, which is comparable to the activation energy we estimate here for Ir(1 1 1) (1.97 eV = ~190 kJ/mol). Based on the D_2O beam flux and surface density, we estimate that probabilities for D_2O dissociation during the scattering experiments are in the range of ~0.0005–0.012 corresponding to the temperature range from 300 to 900 K (as illustrated in Fig. 2b). The percentage uncertainty in dissociation probabilities for D_2O has been estimated to be ~20% of the dissociation probability.

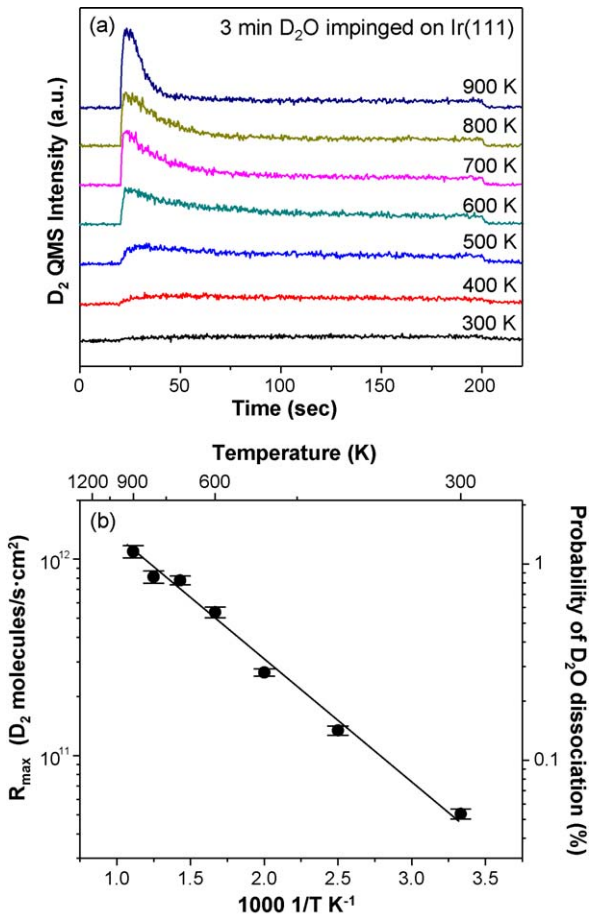

Fig. 2. (a) Evolution of D_2 from 180 s of D_2O impingement on Ir(1 1 1) at various temperatures (300–900 K). (b) Arrhenius plot of maximum D_2 formation rate (R_{max}) regarding the maximum intensity of D_2 (and the probability of D_2O dissociation at R_{max}) during reactive scattering experiments at various temperatures.

We selected the experiment with a sample surface temperature of 900 K (shown as the red curve in Fig. 3), to provide additional insights regarding D_2 evolution from water dissociation. Firstly, we carried out a control experiment (see the black curve in Fig. 3) by

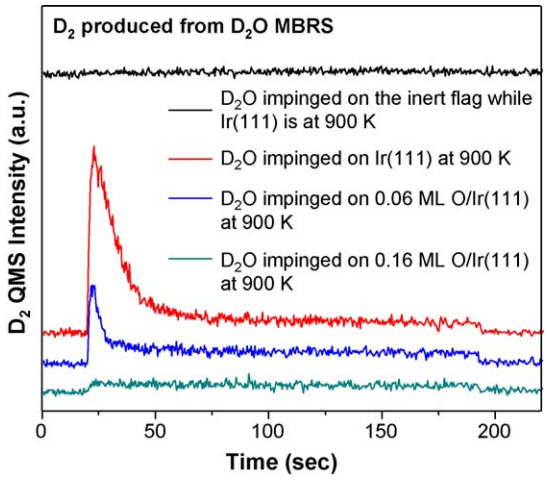

Fig. 3. Evolution of D_2 from 180 s of D_2O impingement on the inert flag (black curve), clean Ir(1 1 1) (red curve), 0.06 ML (blue curve) and 0.16 ML O (green curve) pre-covered Ir(1 1 1) while the Ir(1 1 1) surface temperature was held at 900 K. Oxygen was dosed on the surface between 89 and 77 K. (For interpretation of the references to colour in this figure legend, the reader is referred to the web version of the article.)

impinging a D_2O molecular beam (t = 180 s) onto the stainless steel inert flag placed in front of the Ir(1 1 1) surface while the temperature was held at 900 K. A negligible amount of D_2 production was observed, suggesting that the catalytic activity for thermal dissociation of water under UHV conditions shown in the red curve is due to the Ir(1 1 1) surface. The red curve shows a prompt evolution of D_2 upon exposure to the D_2O beam with the Ir(1 1 1) sample held at 900 K. The decline in the evolution of D_2 during the scattering experiment shown as the red curve in Fig. 3 is likely due to an accumulation of oxygen adatoms from water dissociation gradually populating and blocking the active sites for further water dissociation on Ir(1 1 1) eventually reaching an equilibrium between production and desorption of hydrogen and removal of oxygen (oxygen could be abstracted by background CO and replenished by water). To examine this hypothesis, we scattered an equivalent amount of D_2O (the same flux and dosing time of D_2O to that in the experiment shown in the red curve in Fig. 3) on 0.06 and 0.16 ML oxygen pre-covered Ir(1 1 1) at 900 K, respectively, as the blue and green curves displayed in Fig. 3. With increasing oxygen coverage, the initial D_2 evolution peak is smaller and gradually decreases with a similar amount of D_2 being observed at steady state (compared to the clean surface), supporting our earlier speculation.

3.2. Partial dissociation of water on O pre-covered Ir(1 1 1)

Water dissociation has been observed on many oxygen modified transition metal surfaces, however, details of the interaction between water and oxygen on the Ir(1 1 1) surface have not been reported. In order to study this phenomenon on Ir(1 1 1), we co-adsorbed oxygen (^{16}O) with isotopically labeled water ($H_2{}^{18}O$) to search for the scrambled products (indicators of interaction), such as $^{18}O^{16}O$, $^{18}O_2$ and $H_2{}^{16}O$. Fig. 4 shows TPD spectra of oxygen and water desorbing from the Ir(1 1 1) surface in three separate experiments. Firstly, Fig. 4a and b displays desorption of water and oxygen from 0.30 ML ^{16}O covered Ir(1 1 1) (O_2 is dissociatively chemisorbed on the clean Ir(1 1 1) surface [49,50]). As expected no water is observed desorbing but oxygen desorbs from 1000 to 1400 K in agreement with what Weinberg and co-workers have reported [51,52], where they argued that the 1300 K desorption feature is due to iridium oxide [formed at a temperature higher than ~700 K on the oxygen covered Ir(1 1 1) surface] decomposition. Water TPD spectra on the clean Ir(1 1 1) surface display two features as shown in Fig. 5, with one desorption peak at 160 K due to the multilayer adsorption and the other feature at 170 K for the monolayer adsorption. Fig. 4c exhibits only the monolayer desorption feature (170 K) as the Ir(1 1 1) surface received a relatively small exposure of isotopically labeled water (0.28 ML). Mass 18 was observed to desorb at 170 K also, which is likely due to $H_2{}^{16}O$ impurities in the $H_2{}^{18}O$ sample (Isotec, 95% ^{18}O) or a mass fragment of $H_2{}^{18}O$ or water ($H_2{}^{16}O$) from the background. Notice that there is no oxygen (m/e = 32, 34, 36) desorbing from the Ir(1 1 1) surface covered exclusively by water ($H_2{}^{18}O$), as shown in Fig. 4d. This finding suggests that oxygen atoms from any water dissociation could be totally consumed by reacting with adsorbed trace carbon (from dissociation of hydrocarbon diffusion pump fluid vapor) to form CO and/or CO_2 even on the extremely clean Ir(1 1 1) surface, as the low probability of water dissociation (~0.012) cannot provide detectable oxygen (monitored by QMS) desorbing in the presence of surface carbon contaminants.

In order to study the interaction of water with oxygen on Ir(1 1 1), we added 0.28 ML $H_2{}^{18}O$ to 0.30 ML ^{16}O pre-covered Ir(1 1 1) in a temperature range of 89–77 K, and then carried out TPD measurements. The results illustrated in Fig. 4e show that a new water desorption feature appears at a higher temperature

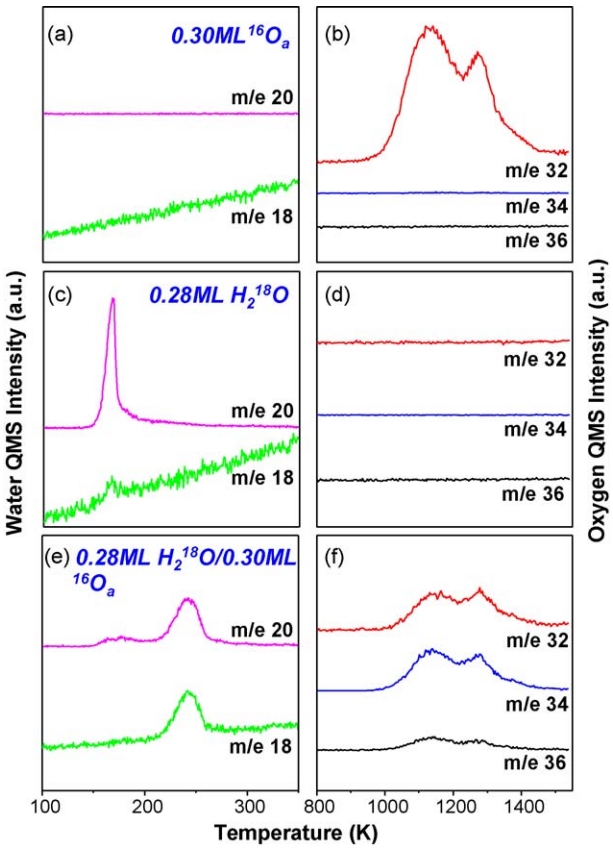

Fig. 4. TPD spectra of water ($H_2{}^{18}O$ and $H_2{}^{16}O$) and oxygen ($^{16}O_2$, $^{16}O^{18}O$ and $^{18}O_2$) from (a) and (b) 0.30 ML ^{16}O on Ir(1 1 1), (c) and (d) 0.28 ML $H_2{}^{18}O$ on Ir(1 1 1), and (e) and (f) 0.28 ML $H_2{}^{18}O$ on 0.30 ML ^{16}O pre-covered Ir(1 1 1). All species were dosed on the surface at 89–77 K. The heating rate during TPD was 2 K/s in the range of 77–500 K and 10 K/s in the range of 500–1550 K.

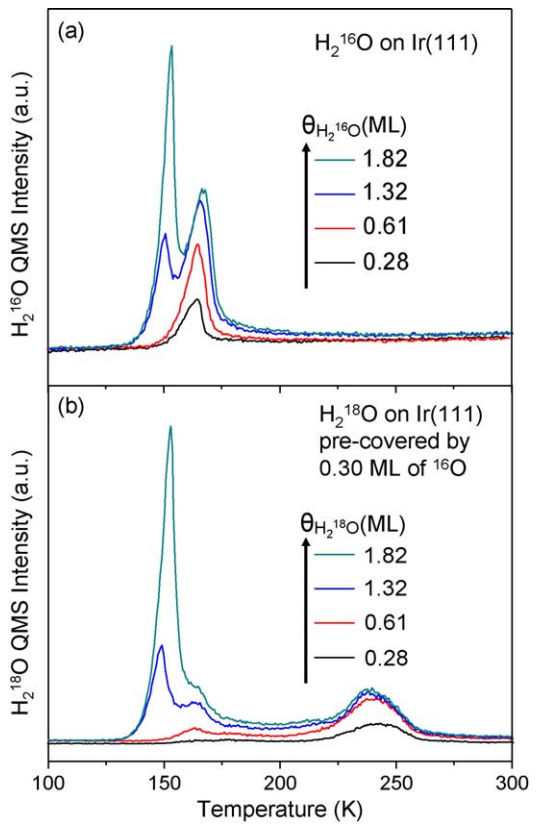

Fig. 6. TPD spectra of $H_2{}^{16}O$ desorption from (a) various $H_2{}^{16}O$ coverages on Ir(1 1 1) and $H_2{}^{18}O$ desorption from (b) various $H_2{}^{18}O$ coverages on 0.30 ML of ^{16}O pre-covered Ir(1 1 1). All species were dosed on the surface at 89–77 K and the heating rate during TPD was 2 K/s.

(235 K). This result likely indicates enhanced water partial dissociation on oxygen covered Ir(1 1 1) forming a hydroxyl group (OH) and leading to a high-temperature water desorption feature due to disproportionation ($2OH_a \rightarrow O_a + H_2O_a$) [53]. Moreover, the notable decrease of the $H_2{}^{18}O$ desorption peak at a low temperature (170 K) suggests that most of the adsorbed water has a strong interaction with atomic oxygen on Ir(1 1 1) at low temperatures as shown in Fig. 4e. Accordingly, the oxygen TPD spectra in Fig. 4f containing

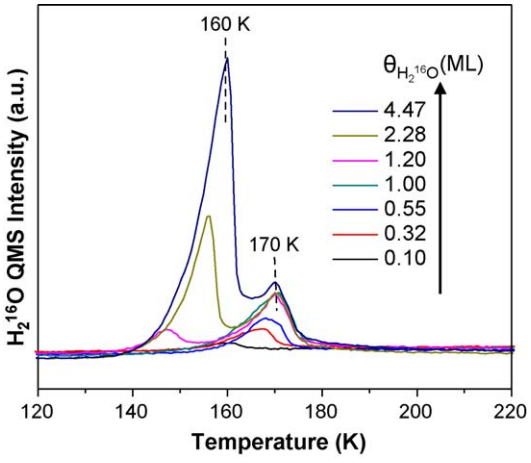

Fig. 5. TPD spectra of $H_2{}^{16}O$ desorption from various water coverages on Ir(1 1 1). Water was dosed on the surface between 89 and 77 K and the heating rate was 2 K/s.

m/e = 32, 34, and 36 provide evidence regarding oxygen scrambling between oxygen and water also due to disproportionation of formed OH groups. We believe that this process follows the widely accepted mechanism of hydrogen abstraction to produce hydroxyl groups, in which the co-adsorbed atomic oxygen induces water dissociation by abstracting hydrogen atoms from adsorbed water molecules ($O_a + H_2O_a \rightarrow 2OH_a$) [53]. When we further increase the $H_2{}^{18}O$ coverage on 0.30 ML of oxygen pre-covered Ir(1 1 1), more recombined water and scrambled oxygen ($^{16}O^{18}O$ and $^{18}O_2$) are produced while the desorption of multilayer water also can be observed with increasing water coverages as shown in Fig. 6.

We have found enhancement by oxygen adatoms for partial dissociation of water on Ir(1 1 1) (see Fig. 4) and also speculated that oxygen from D_2O dissociation could populate the sample surface and block the active sites for further complete dissociation during scattering experiments as shown in Fig. 3. A small amount of water dissociates in the low temperature experiments with the probability ranging from ~0.004 to 0.016 and in the molecular beam reactive scattering measurements with probabilities in the range of ~0.0005–0.012, and this suggests that the water dissociation (detected via hydrogen evolution) observed on the clean Ir(1 1 1) surface could be due to a small concentration of defects or trace surface carbon contamination whereas clearly a strong interaction between water and oxygen occurs (detected via scrambling) on the (1 1 1) terraces. In order to investigate the effect of carbon, we dosed propylene on the clean Ir(1 1 1) surface via molecular beam and then heated the sample to 900 K to obtain ~4.5 times more carbon on Ir(1 1 1) than the "clean" surface. However, D_2O scattering experiments on carbon pre-covered Ir(1 1 1) showed that only 10% larger peak value of D_2 was detected than that on the clean surface,

indicating carbon is not likely responsible for water dissociation. Although more D_2 production has been observed on carbon precovered surface during the steady state, we believe that it is because the rate of O blocking active site (i.e. defects) has been decreased by CO oxidation which can consume oxygen atoms and suppress their population on Ir(1 1 1). Therefore, we suspect that water dissociation on the clean Ir(1 1 1) surface is mediated by defects [9,53] (the water dissociation probability on Ir(1 1 0) is ~6% [38]). The defective sites are likely blocked by oxygen atoms from dissociated water causing the attenuation of further dissociation and evolution of D_2. On the other hand, oxygen atoms can enhance *partial* dissociation of water on the (1 1 1) terraces of our iridium sample via abstraction of H. Additionally, complete dissociation of D_2O on defects of Ir(1 1 1) might result in the desorption of D_2 at the higher temperatures (up to ~600 K) as shown in Fig. 1, compared to the D_2 TPD spectra reported by Engstrom and Weinberg (hydrogen and deuterium desorption features are identical and end at ~500 K on Ir(1 1 1) terraces [46]). The broader TPD spectra for deuterium in our work could be due to the different source for D_2, i.e., produced from water dissociation whereas Weinberg and co-workers directly adsorbed deuterium for their TPD measurements.

Comparing the probability of water dissociation in TPD ($0.004–0.016 \pm 0.0015$) and scattering (0.0005–0.012 with a 20% uncertainty) experiments, we have noted that slightly larger fractions of D_2O molecules can completely dissociate on the clean Ir(1 1 1) surface in TPD. As the adsorption probability is likely only affected in a minor way by surface temperature [30], the difference in water dissociation probability for the two types of measurements (TPD and MBRS) might be due to the residence time of the molecules. The longer residence time of water molecules at low temperature (approaching infinity at 77 K) in TPD allows D_2O molecule to diffuse to active sites and dissociate with a large number of attempts. As a result, a higher probability of reaction is obtained. In contrast, in the scattering experiments with surface temperatures much higher than that of water desorption a much shorter residence time (ranging from 10^{-6} to 10^{-11} s) is expected so that water molecules cannot repeatedly reach the reactive sites as desorption is quite rapid, and this results in a comparably lower dissociation probability. However, reactivity increases with increasing surface temperature when a D_2O molecular beam is impinged on Ir(1 1 1), indicating that complete dissociation of water is thermally activated at temperatures above 300 K and mainly influenced by reaction probability rather than probability of molecules arriving at the defective sites. Additionally, a crude calculation of D_2O coverage shows it to be very small (10^{-7} to 10^{-12} monolayer) during the scattering experiments with the temperatures ranging from 300 to 900 K.

The role of a trace amount of moisture in increasing reaction rates in high surface area catalysis, has been identified in investigations regarding CO oxidation [26] and propylene epoxidation [54] on supported gold clusters. The data presented here aim to reinforce the understanding of the role of adsorbed water with clean and oxygen modified Ir(1 1 1).

4. Conclusions

In summary, water dissociation has been observed on the clean Ir(1 1 1) surface via TPD with a small dissociation probability (lower than $\sim 0.016 \pm 0.0015$). Using molecular beam reactive scattering techniques, we found that water dissociation on Ir(1 1 1) is activated whereas adsorbed oxygen produced from the reaction can occupy the active sites to inhibit the further dissociation of water causing dissociation probabilities in a range of ~0.0005–0.012 (20% uncertainty) at the maximum reaction rate. Furthermore, the apparent activation energy has been estimated to be $\sim 170 \pm 5$ kJ/mol, which may not be applicable to the higher coverages employed for the TPD measurements. When water and oxygen were co-adsorbed on Ir(1 1 1), scrambled products were detected, suggesting that oxygen can induce partial dissociation of water on Ir(1 1 1) and recombinative desorption in which hydroxyl groups are considered to be likely intermediates. A new prominent desorption feature at 235 K, which is at a much higher temperature than the characteristic desorption feature for monolayer water on clean Ir(1 1 1) (170 K), suggests a strong interaction between oxygen and water.

Acknowledgements

We thank the Department of Energy (DE-FG02-04ER15587), the Welch Foundation(F-1436), and the National Science Foundation (CTS-0553243) for their support.

References

[1] R.T. Kinch, C.R. Cabrera, Y. Ishikawa, J. Phys. Chem. C 113 (2009) 9239.
[2] A.A. Gokhale, J.A. Dumesic, M. Mavrikakis, J. Am. Chem. Soc. 130 (2008) 1402.
[3] H. Torninaga, M. Nagai, Appl. Catal. A: Gen. 328 (2007) 35.
[4] D.W. Blaylock, T. Ogura, W.H. Green, G.J.O. Beran, J. Phys. Chem. C 113 (2009) 4898.
[5] K. Andersson, A. Nikitin, L.G.M. Pettersson, A. Nilsson, H. Ogasawara, Phys. Rev. Lett. 93 (2004) 196101.
[6] N.S. Faradzhev, K.L. Kostov, P. Feulner, T.E. Madey, D. Menzel, Chem. Phys. Lett. 415 (2005) 165.
[7] P.J. Feibelman, Science 295 (2002) 99.
[8] T. Jacob, W.A. Goddard, J. Am. Chem. Soc. 126 (2004) 9360.
[9] A.A. Phatak, W.N. Delgass, F.H. Ribeiro, W.F. Schneider, J. Phys. Chem. C 113 (2009) 7269.
[10] B. Li, K. Griffiths, C.S. Zhang, P.R. Norton, Surf. Sci. 384 (1997) 70.
[11] A.F. Carley, S. Rassias, M.W. Roberts, Surf. Sci. 135 (1983) 35.
[12] G.-C. Wang, S.-X. Tao, X.-H. Bu, J. Catal. 244 (2006) 10.
[13] B. Atsushi, Y. Susumu, M. Kozo, Y. Yoshiyuki, Y. Jun, J. Chem. Phys. 125 (2006) 054717.
[14] K.D. Gibson, M. Viste, S.J. Sibener, J. Chem. Phys. 112 (2000) 9582.
[15] C. Ammon, A. Bayer, H.P. Steinrück, G. Held, Chem. Phys. Lett. 377 (2003) 163.
[16] L. Guillemot, K. Bobrov, Surf. Sci. 601 (2007) 871.
[17] R.G. Quiller, T.A. Baker, X. Deng, M.E. Colling, B.K. Min, C.M. Friend, J. Chem. Phys. 129 (2008) 064702.
[18] K. Bange, D.E. Grider, T.E. Madey, J.K. Sass, Surf. Sci. 137 (1984) 38.
[19] C. Benndorf, C. Nöbl, F. Thieme, Surf. Sci. 121 (1982) 249.
[20] P. Cabrera-Sanfelix, A. Arnau, A. Mugarza, T.K. Shimizu, M. Salmeron, D. Sanchez-Portal, Phys. Rev. B 78 (2008) 5.
[21] M.J. Gladys, A. Mikkelsen, J.N. Andersen, G. Held, Chem. Phys. Lett. 414 (2005) 311.
[22] H.S. Guo, F. Zaera, Catal. Lett. 88 (2003) 95.
[23] R.A. Ojifinni, N.S. Froemming, J. Gong, M. Pan, T.S. Kim, J.M. White, G. Henkelman, C.B. Mullins, J. Am. Chem. Soc. 130 (2008) 6801.
[24] T.S. Kim, J. Gong, R.A. Ojifinni, J.M. White, C.B. Mullins, J. Am. Chem. Soc. 128 (2006) 6282.
[25] J. Bergeld, B. Kasemo, D.V. Chakarov, Surf. Sci. 495 (2001) L815.
[26] M. Date, M. Haruta, J. Catal. 201 (2001) 221.
[27] M. Date, M. Okumura, S. Tsubota, M. Haruta, Angew. Chem. Int. Ed. 43 (2004) 2129.
[28] J.T. Ranney, S.R. Bare, J.L. Gland, Catal. Lett. 48 (1997) 25.
[29] M. Pan, S. Hoang, J. Gong, C.B. Mullins, Chem. Commun. (2009) 7300.
[30] G.O. Sitz, C.B. Mullins, J. Phys. Chem. B 106 (2002) 8349.
[31] M.C. Wheeler, C.T. Reeves, D.C. Seets, C.B. Mullins, J. Chem. Phys. 108 (1998) 3057.
[32] S.G. Karseboom, J.E. Davis, C.B. Mullins, Surf. Sci. 383 (1997) 173.
[33] D.C. Seets, M.C. Wheeler, C.B. Mullins, Chem. Phys. Lett. 266 (1997) 431.
[34] W.J. Cai, F.G. Wang, E.S. Zhan, A.C. Van Veen, C. Mirodatos, W.J. Shen, J. Catal. 257 (2008) 96.
[35] Y. Sato, Y. Soma, T. Miyao, S. Naito, Appl. Catal. A: Gen. 304 (2006) 78.
[36] C.J. Hagedorn, M.J. Weiss, T.W. Kim, W.H. Weinberg, J. Am. Chem. Soc. 123 (2001) 929.
[37] D. Kelly, W.H. Weinberg, J. Chem. Phys. 105 (1996) 11313.
[38] T.S. Wittrig, D.E. Ibbotson, W.H. Weinberg, Surf. Sci. 102 (1981) 506.
[39] J.E. Davis, S.G. Karseboom, P.D. Nolan, C.B. Mullins, J. Chem. Phys. 105 (1996) 8362.
[40] B.A. Ferguson, C.T. Reeves, C.B. Mullins, J. Chem. Phys. 110 (1999) 11574.
[41] P.D. Nolan, B.R. Lutz, P.L. Tanaka, J.E. Davis, C.B. Mullins, J. Chem. Phys. 111 (1999) 3696.
[42] P.D. Nolan, B.R. Lutz, P.L. Tanaka, J.E. Davis, C.B. Mullins, Phys. Rev. Lett. 81 (1998) 3179.
[43] P.D. Nolan, B.R. Lutz, P.L. Tanaka, C.B. Mullins, Surf. Sci. 419 (1998) L107.
[44] T.S. Marinova, K.L. Kostov, Surf. Sci. 185 (1987) 203.

[45] A. Picolin, C. Busse, A. Redinger, M. Morgenstern, T. Michely, J. Phys. Chem. C 113 (2009) 691.
[46] J.R. Engstrom, W. Tsai, W.H. Weinberg, J. Chem. Phys. 87 (1987) 3104.
[47] P.A. Thiel, T.E. Madey, Surf. Sci. Rep. 7 (1987) 211.
[48] L.C. Grabow, A.A. Gokhale, S.T. Evans, J.A. Dumesic, M. Mavrikakis, J. Phys. Chem. C 112 (2008) 4608.
[49] J.E. Davis, P.D. Nolan, S.G. Karseboom, C.B. Mullins, J. Chem. Phys. 107 (1997) 943.
[50] P.D. Nolan, M.C. Wheeler, J.E. Davis, C.B. Mullins, Acc. Chem. Res. 31 (1998) 798.
[51] V.P. Ivanov, G.K. Boreskov, V.I. Savchenko, W.F. Egelhoff, W.H. Weinberg, Surf. Sci. 61 (1976) 207.
[52] P.A. Zhdan, G.K. Boreskov, A.I. Boronin, W.F. Egelhoff Jr., W.H. Weinberg, Surf. Sci. 61 (1976) 25.
[53] M.A. Henderson, Surf. Sci. Rep. 46 (2002) 1.
[54] J.T. Ranney, J.L. Gland, S.R. Bare, Surf. Sci. 401 (1998) 1.